APPLICATION OF THE GRA^{MC} MESH-HANDLING STRATEGY FOR THE SIMULATION OF DIP AND INJECTION LUBRICATION IN GEARBOXES

MARCO NICOLA MASTRONE & FRANCO CONCLI
Free University of Bolzano, Italy.

ABSTRACT

Computer-aided engineering (CAE) refers to software applications aimed at helping solve technological problems through numerical methods. Exploiting CAE, it is possible to evaluate determined systems through virtual models rather than physical prototypes. By doing so, useful information on the system's performance can be gathered at the beginning of the design phase, when the modifications to the project cost less. In the field of lubrication and efficiency, computational fluid dynamics (CFD) has been applied to geared transmissions, leading to an important step forward in the understanding of multiphase physics and the optimization of the systems' layout. Being the simulations of gears nonstationary, the topological changes of the domain require the adoption of mesh-handling strategies capable of accomplishing the boundaries' rotation. In this analysis, the Global Remeshing Algorithm with Mesh Clustering (GRA^{MC}), previously developed by the authors to reduce the computational time associated with the remeshing process, is applied to study dip and injection lubrication in helical and spur gearboxes. The results suggest that this methodology is an effective and efficient solution to analyse the lubrication and the efficiency even for complex kinematics. The investigation was conducted in the OpenFOAM framework.
Keywords: CFD, efficiency, gears, lubrication, mesh handling, OpenFOAM, power losses.

1 INTRODUCTION

Mechanical design has hugely benefitted from the signs of progress in computer sciences, not only regarding the computational power of HPCs but also in the availability of more and more sophisticated numerical tools, namely, software packages. In this sense, computer-aided engineering (CAE) is nowadays widely used in academia and industry to approach typical engineering problems, e.g. finite element analysis (FEA) for structural problems and computational fluid dynamics (CFD) for fluid dynamics problems. Virtual modelling enables the investigation of systems without the need for physical prototypes, thus bringing clear advantages in the design phase of a product. The design and optimization of gearboxes could be tackled by numerical tools. In particular, the efficiency and the lubricant fluxes in the transmissions, which play a determinant role in the lifetime of the components of the whole system, can be predicted by exploiting CFD codes. By doing so, it is also possible to have a better comprehension of the physics involved and even to understand the local performance of a component.

However, the massive application of these codes in the industry is limited by the computational costs of the dynamic mesh management and the computational resources needed in terms of hardware requirements. Indeed, the distortion of the grid's elements during the wheels' rotation requires the user to adopt specific mesh-handling strategies to guarantee that the elements' quality is enough to ensure the solution convergence.

While in the CFD simulation of spur gears, the remeshing problem can be reduced to a 2.5D problem (the whole 3D mesh can be created with a series of extrusions starting from a

2D plane) [1–10], and complex domains such as bevel and helical gears must be meshed with tetrahedrons (and not with triangular prisms as for spur gears). Tetrahedral meshes are characterized by higher generation times with respect to prismatic or hexahedral elements. Single rotating helical gears [11] and spiral bevel gears [12] have been already simulated by the authors, while the virtual modelling of mating gears has been approached with mesh [13–20] and meshless methods [21–26] in commercial software. Works based on a general procedure in open-source software are still lacking in the literature. Therefore, the authors believe that the introduction of advanced mesh-handling strategies would have significant benefits for the efficient simulation of mating gears. In this work (an extension of the results presented at a conference [27]), the Global Remeshing Approach with Mesh Clustering (GRA^{MC}), already used by the authors to study its effectiveness [28, 29], is applied to study dip lubrication in a helical gearbox and injection lubrication in a spur gearbox. This work is aimed at showing, on the one hand, the significance of the proposed remeshing strategy to reduce the computational effort of these types of simulations, and on the other hand, the information that can be extracted from such analyses. The methodology is implemented in the open-source framework OpenFOAM® [30].

2 MATERIALS AND METHODS

2.1 Meshing strategy

The mesh generators that can be found in OpenFOAM® are blockMesh and snappyHexMesh. These applications build hex-dominant meshes but are characterized by some disadvantages for the simulation of gears. In fact, blockMesh would require intricate partitions of the gearbox geometry for every little angular rotation of the wheels, and is therefore not suitable in this context; snappyHexMesh, on the other hand, can work in principle, but the high time and memory requirements make this application unsuitable for the gears application. External meshing software can be used as well. The mesh will then need to be converted to the OpenFOAM® format. In this work, Salome [31] is exploited for mesh generation. Due to the wheels' rotations, a valid grid must be ensured at every angular step. This requirement translates into the necessity to provide a new valid mesh every time the previous mesh loses its angular validity in terms of quality indicators. Therefore, mesh generation represents a fundamental aspect that must be carefully considered in intersecting dynamic domains like gears. Indeed, if the mesh-handling strategy is not performant, the simulations cannot be managed in a reasonable amount of time because of the high computational effort.

The GRA^{MC} was developed with the objective of minimizing the remeshing time of complex domains and physics by exploiting the cyclicality of the gear position. By doing so, once the numerical meshes covering one engagement have been computed, they can be 'recycled' for the whole simulation. This algorithm requires the correct setup of the time libraries in order to ensure that the gears find themselves in the computed mesh positions at the end of each angular step. This strategy allowed a significant reduction in the simulation time for domains that would suffer from severe computational problems (such as helical and bevel gearboxes), demonstrating its flexibility and applicability in many geometries.

The calculation of the minimum number of grids that can cover the deformation of one engagement is accomplished with a pre-simulation, in which only the nodal displacements are solved, not the field variables such as pressure and velocity. This allows a fast evaluation of the deformation that a mesh can undergo before the deterioration of its computational

elements. Being ø the angle between two teeth, N_{teeth} the number of the gears' teeth, ω the rotational speed of the wheels, N_{up} the mesh updating time, and T_{eng} and N_{mesh} the time and the number of meshes needed to perform one engagement, the relationships that allow the generation of the minimum number of grids are the following:

$$\phi = \frac{2\pi}{N_{\text{teeth}}} \tag{1}$$

$$T_{\text{eng}} = \frac{\phi}{\omega} \tag{2}$$

$$N_{\text{mesh}} = \frac{T_{\text{eng}}}{t_{\text{up}}} \tag{3}$$

The algorithm foresees the interpolation of the results from grid to grid. The consistent mapping option is adopted to ensure that the interpolation occurs between conformal geometries. The fact that the user has direct control over the mesh generation procedure enables the reduction of the interpolation errors; the mesh size, in fact, is almost the same for all meshes. When the regime is reached (i.e. when the fluid dynamic forces stabilize around a mean value with small fluctuations around the gear meshing frequency), the post-processing of the results provides information about the lubrication and the efficiency of the transmission. The whole process is implemented in a Bash [32] script. With this strategy, the computational effort related to the mesh management is reduced significantly; indeed, once the mesh set is available, every grid is immediately provided at each necessary substitution during the wheels' rotation. The time attributable to the 'mesh' part of the algorithm is reduced to the results' interpolation from mesh to mesh. A set of 10 and 15 grids was used for the helical and the spur gearbox, respectively. This allowed a reduction of about 95% of the time ascribable to the mesh, and about 15% (spur gears) and 70% (helical gears) of the total simulation time with respect to a standard remeshing approach.

2.2 Numerical approach

In the analysed cases, the simulations were considered isothermal. Therefore, the energy equation was not activated, and the conservation equations of mass and momentum were solved by the CFD code:

$$\frac{\partial \rho}{\partial t} + \nabla(\rho \boldsymbol{u}) = 0 \tag{4}$$

$$\frac{\partial(\rho \boldsymbol{u})}{\partial t} + \nabla(\rho \boldsymbol{u}\boldsymbol{u}) = -\nabla p + \nabla\left[\mu\left(\nabla \boldsymbol{u} + \nabla \boldsymbol{u}^T\right)\right] + \rho \boldsymbol{g} + \boldsymbol{F} \tag{5}$$

Since these equations are valid only in monophasic simulations, a third conservation equation is added to account for two fluids. The VOF model [33] is used. The equation of the volumetric fraction (percentage of one fluid in every cell of the domain) is the following:

$$\frac{\partial \alpha}{\partial t} + \nabla(\alpha \boldsymbol{u}) = 0 \tag{6}$$

A generic physical property Θ (like viscosity and density) of the two fluids is used to describe an equivalent fluid such that:

$$\Theta_{eq} = \Theta_1 \cdot \alpha + \Theta_2 \cdot (1 - \alpha) \tag{7}$$

The value of α can assume values between 0 and 1. In order to guarantee a bounded solution, the compressive scheme MULES (Multidimensional Universal Limiter with Explicit Solution) [34] was used. The MULES improves the interface resolution by the addition of the relative velocity $\boldsymbol{u}_c$ that, by acting perpendicularly to the interface, estimates the relative velocity between fluids. The equation of α becomes:

$$\frac{\partial \alpha}{\partial t} + \nabla(\alpha \boldsymbol{u}) + \nabla(\boldsymbol{u_c}\alpha(1 - \alpha)) = 0 \tag{8}$$

The further addition of a source term to the right part of the equation (S_g) permits the inclusion of physical phenomena such as aeration and cavitation:

$$\frac{\partial \alpha}{\partial t} + \nabla(\alpha \boldsymbol{u}) + \nabla(\boldsymbol{u_c}\alpha(1 - \alpha)) = S_g \tag{9}$$

In this work, cavitation is modelled according to the Kunz model [35]. The great advantage of this expression is related to the fact that the source term is independent of the pressure. The vaporization ($\dot{m}_v$) is modelled as proportional to the liquid fraction (α) and to the quantity of pressure under the saturation pressure (p_{sat}). The condensation ($\dot{m}_c$) is modelled analogously:

$$\dot{m}_v = \frac{C_v \rho_v}{\frac{1}{2}\rho_l U_\infty^2 t_\infty} \alpha \min[0, p - p_{sat}] \tag{10}$$

$$\dot{m}_c = \frac{C_c}{\frac{1}{2}U_\infty^2 t_\infty} (1 - \alpha)\max[0, p - p_{sat}] \tag{11}$$

2.3 Analysed systems

Two systems were studied with the GRA^{MC}: a helical gearbox (whose design parameters are reported in Table 1) and a spur gearbox (whose design parameters are reported in Table 2).

In both systems, the wheels were scaled to 99% of their actual size (only in the radial direction, not in the axial one). This ensures a small gap between the teeth where valid computational cells can be generated.

The minimum elements' size was set to 1 mm in the gears' region, while a global size of 5 mm was imposed in the region moving toward the walls of the box (a growth rate between cells of 20%). With these settings, the set resulted in high-quality meshes for both configurations. The total number of cells is about 520K for the helical gearbox and about 400K cells for the spur gearbox. The mesh of the wheels is reported in Fig. 1.

In Table 3, the simulated operating conditions are reported.

Table 1: Helical gearbox.

	Unit	Gears
Transmission ratio	–	1
Number of teeth	–	23
Module	mm	4
Helix angle	°	27
Face width	mm	40

Table 2: Spur gearbox.

	Unit	Gears
Transmission ratio	–	1.5
Number of teeth	–	24–16
Module	mm	4.5
Helix angle	°	0
Face width	mm	14

a)   b)
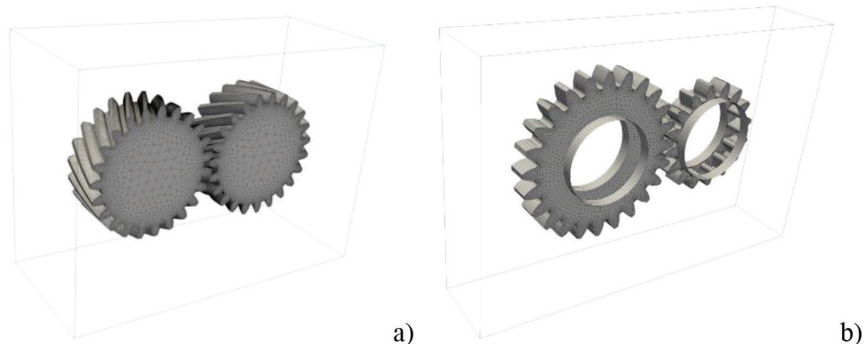
Figure 1: Numerical mesh: (a) helical gears (tetrahedrons) and (b) spur gears (triangular prisms).

2.4 Numerical schemes

The PIMPLE algorithm was adopted to solve the transient simulations. Two correctors of the pressure equation were imposed to maintain the stability of the solution. A convergence criterion of 1e-6 was imposed on all the field variables. The PCG (preconditioned conjugate gradient) solver was used for the pressure. The velocity was solved with the PBiCG (stabilized preconditioned bi-conjugate gradient). The timestep was set to achieve a maximum Courant number of 1. The time derivative was discretized with the first-order implicit Euler scheme, the velocity with the second-order *linearUpwind* scheme, and the convection of the volumetric fraction with the *vanLeer* scheme.

Table 3: Operating conditions.

	Operating condition	Rotational speed pinion (rpm)	Oil density (kg/m³)	Oil viscosity (mm²/s)
Helical gears	Multiphase (centerline)	3000	800	0.001
		6000		
	Complete filling	3000		
		6000		
	Complete filling with cavitation	3000		
		6000		
Spur gears	Injection lubrication	1150		
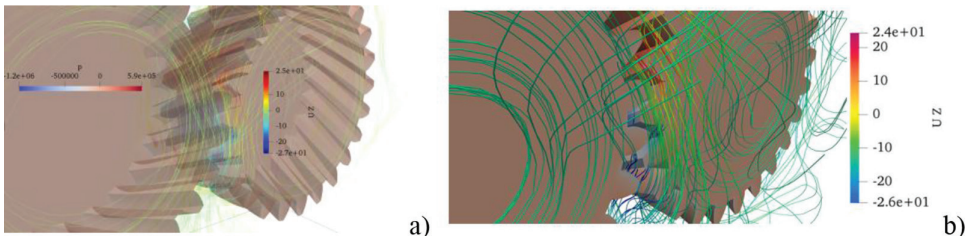
Figure 2: Axial velocity streamlines and pressure contour in the meshing zone.

3 RESULTS

3.1 Helical gearbox

In Fig. 2a, the axial velocity streamlines (U_z) together with the pressure contour in the engagement are illustrated for the complete filling case without cavitation (pressurization was applied to ensure the complete wheels' wetting). It can be noted that the pressure gradient promotes both squeezing and suction effects, which is emphasized by the detailed view of the axial velocity streamlines (positive before the pitch point and negative after it) in Fig. 2b.

Figure 3 shows the pressure distribution on the gear's flanks for the cavitation case. With the pressure limited to the vaporization pressure, the typical negative pressure peaks of the windage effects are not present since that region is cavitating. The inclusion of a cavitation model in the simulations was necessary to physically explain the experimental evidence observed in ref. [36]. In fact, the measured power losses are lower with respect to the ones measured in the case of complete filling with applied pressurization. Since the pressure is hydrostatic, it should not affect the resistant torque. With the experimental findings in contrast with these considerations, the only way to explain the difference in the efficiency is to admit a phase change from liquid to vapor. By doing so, the pressure is limited to a positive minimum, thus leading to lower power dissipation.
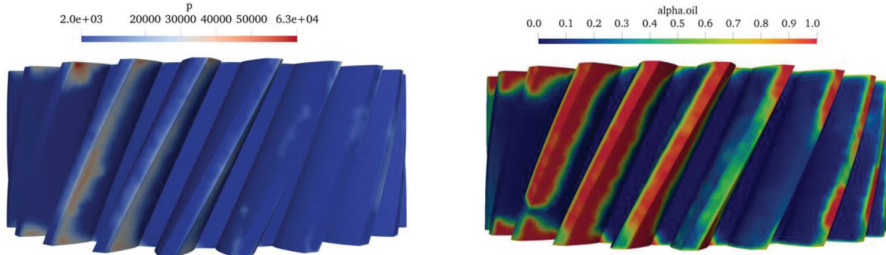
Figure 3: Pressure and volumetric fraction on the wheel (cavitation case).
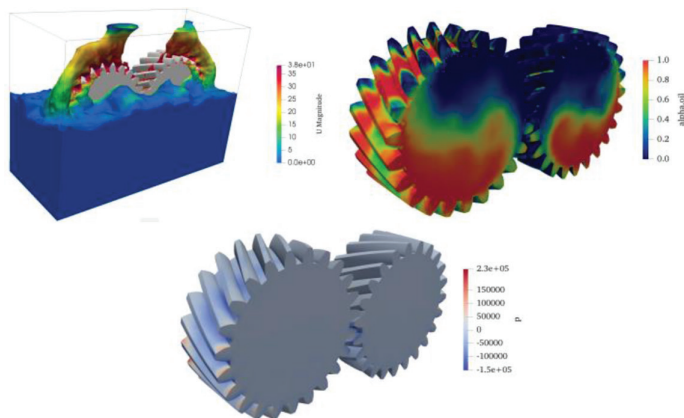
Figure 4: Lubricant distribution in the gearbox, volumetric fraction contour on the wheels, and pressure contour.

In Fig. 4, the lubricant distribution for the multiphase case at 6000 rpm is shown. It can be noticed that the lubricant tends to hit the upper wall of the box and successively fall down in the sump. A certain amount of oil slides along the teeth flanks due to the helical shape of the teeth. The inertial effects of the lubricant generate pressure peaks in the areas in contact with it.

In Fig. 5 the plot of the resistant torque vs. rotational speed is shown. The influence of the three operating conditions on the torque loss can be clearly seen.

3.2 Spur gearbox

The spur gearbox was simulated in case of injection lubrication. An area having the axial length of the gears was modelled as the injection zone. An inlet velocity four times higher than the tangential speed of the pinion was used for the simulation. The oil distribution during the injection is reported in Fig. 6.

It can be noticed that the oil enters the gear mesh promoting predominant squeezing effects in the axial direction. The oil is then dragged by the wheels originating rivulets. In this regime, the flanks seem well lubricated.

In Fig. 7, the resistant torque over time is shown. After an initial transitory, the losses stabilize around a mean value, which can be taken as the estimation of the torque loss for the analysed operating condition.
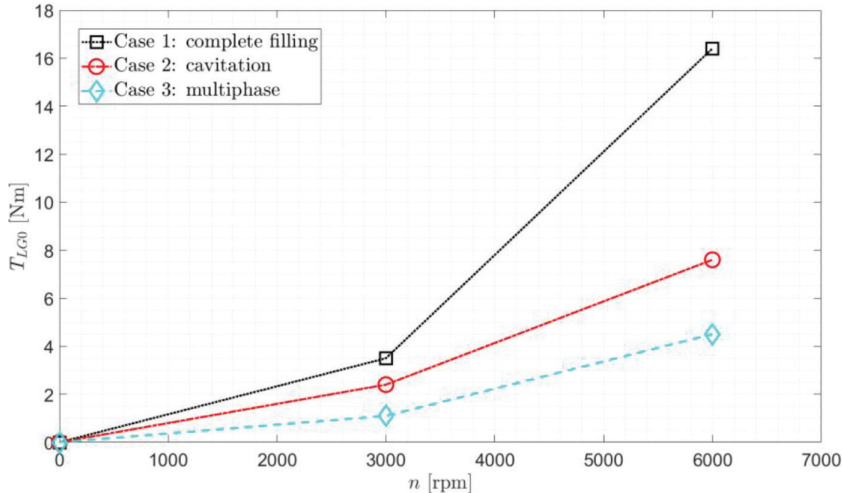
Figure 5: Torque loss vs. rotational speed for the different operating conditions.
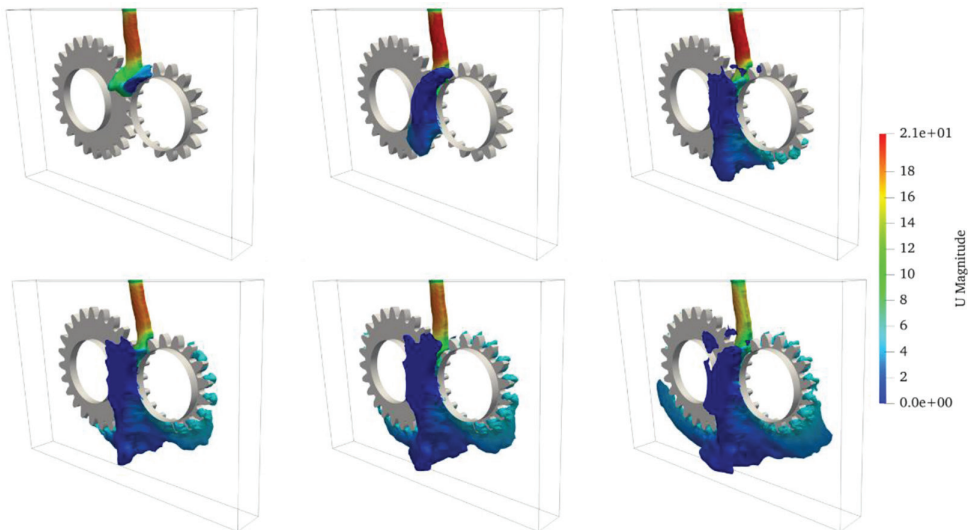

Figure 6: Lubricant distribution during the wheels' rotation.

Considering that, in order to gather this information, experimental tests including a transparent case for the lubricant visualization and a torque meter for the resistant torque measurement would be necessary, the practical implication of the shown numerical analysis can be clearly understood. Moreover, the adopted mesh-handling strategy has the great advantage of reducing the complexity of the remeshing process during the wheel's rotation, making this procedure applicable to various systems and operating conditions.
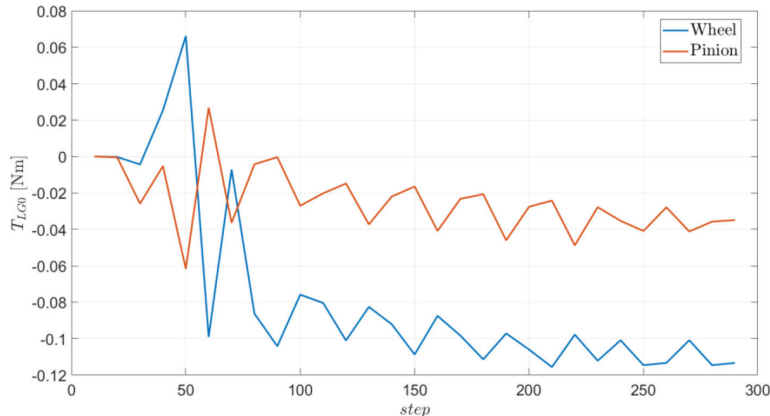
Figure 7: Evolution of the torque loss over the timesteps and stabilization at regime.

4 CONCLUSIONS

In this work, the GRA^MC mesh-handling strategy (previously implemented by the authors in OpenFOAM®) was exploited to study dip lubrication in a helical gearbox and injection lubrication in a spur gearbox. The adopted strategy, which is based on the computation of a limited number of numerical grids (defining the wheels' positions at predefined intervals during the engagement), has proven to be reliable and efficient for such kinds of analysis. The reduction of the simulation time allowed us to study configurations and operating conditions that would not have been negligible with standard remeshing methods in terms of computational effort. The analysis of such simulations allows the designer to obtain information not only in terms of lubricant flow in the transmission but also in terms of efficiency. In particular, efficiency is of primary importance according to the latest international trends and requirements; indeed, efficient solutions translate into environmental savings. This article fits into this sense, showing the potential of the proposed remeshing strategy to gather information on the losses that originate in different operating conditions and, consequently, to optimize the design solution for the specific application of interest.

REFERENCES

[1] Liu, H., Jurkschat, T., Lohner, T. & Stahl, K., Determination of oil distribution and churning power loss of gearboxes by finite volume CFD method. *Tribol. Int.*, vol. **109**, pp. 346–354, 2017. https://doi.org/10.1016/j.triboint.2016.12.042

[2] Mastrone, M.N., Hartono, E.A., Chernoray, V. & Concli, F., Oil distribution and churning losses of gearboxes: Experimental and numerical analysis. *Tribol. Int.*, **151**, 2020. https://doi.org/10.1016/j.triboint.2020.106496

[3] Concli, F., Maccioni, L. & Gorla, C., Lubrication of gearboxes: CFD analysis of a cycloidal gear set. In *WIT Transactions on Engineering Sciences*, **123**, pp. 101–112, 2019. https://doi.org/10.2495/MPF190101

[4] Liu, H., Jurkschat, T., Lohner, T. & Stahl, K., Detailed investigations on the oil flow in dip-lubricated gearboxes by the finite volume CFD method. *Lubricants*, **6(2)**, 2018. https://doi.org/10.3390/lubricants6020047

[5] Mastrone, M.N. & Concli, F., CFD simulation of grease lubrication: Analysis of the power losses and lubricant flows inside a back-to-back test rig gearbox. *J. Nonnewton. Fluid Mech.*, **297**, 2021. https://doi.org/10.1016/j.jnnfm.2021.104652

[6] Burberi, E., Fondelli, T., Andreini, A., Facchini, B. & Cipolla, L., CFD simulations of a meshing gear pair. In *Proceedings of the ASME Turbo Expo*, **5A-2016**, 2016. https://doi.org/10.1115/GT2016-57454

[7] Hildebrand, L., Dangl, F., Sedlmair, M., Lohner, T. & Stahl, K., CFD analysis on the oil flow of a gear stage with guide plate. *Eng. Res.*, 2021. https://doi.org/10.1007/s10010-021-00523-5

[8] Concli, F. & Gorla, C., A CFD analysis of the oil squeezing power losses of a gear pair. *Int. J. Comput. Methods Exp. Meas.*, **2(2)**, pp. 157–167, 2014. https://doi.org/10.2495/CMEM-V2-N2-157-167

[9] Bianchini, C., Da Soghe, R., Errico, J.D. & Tarchi, L., Computational analysis of wind-age losses in an epicyclic gear train. In *Proceedings of the ASME Turbo Expo*, **5B-2017**, 2017. https://doi.org/10.1115/GT2017-64917

[10] Bianchini, C., *et al.*, Load independent losses of an aeroengine epicyclic power gear train: Numerical investigation. In *Proceedings of the ASME Turbo Expo 2019: Turbomachinery Technical Conference and Exposition*, 2019. https://doi.org/10.1115/GT2019-91309

[11] Concli, F., Gorla, C., Della Torre, A. & Montenegro, G., Windage power losses of ordinary gears: different CFD approaches aimed to the reduction of the computational effort. *Lubricants*, **2(4)**, pp. 162–176, 2014. https://doi.org/10.3390/lubricants2040162

[12] Mastrone, M.N. & Concli, F., Power losses of spiral bevel gears: an analysis based on computational fluid dynamics. *Front. Mech. Eng.*, **7**, 2021. https://doi.org/10.3389/fmech.2021.655266

[13] Dai, Y., Ma, F., Zhu, X., Su, Q., & Hu, X., Evaluation and optimization of the oil jet lubrication performance for orthogonal face gear drive: Modelling, simulation and experimental validation. *Energies*, **12(10)**, 2019. https://doi.org/10.3390/en12101935

[14] Ferrari, C. & Marani, P., Study of air inclusion in lubrication system of CVT gearbox transmission with biphasic CFD simulation, 2016.

[15] Hu, X., Jiang, Y., Luo, C., Feng, L. & Dai, Y., Churning power losses of a gearbox with spiral bevel geared transmission. *Tribol. Int.*, **129**, pp. 398–406, 2019. https://doi.org/10.1016/j.triboint.2018.08.041

[16] Peng, Q., Zhou, C., Gui, L. & Fan, Z., Investigation of the lubrication system in a vehicle axle: Numerical model and experimental validation. *Proc. Inst. Mech. Eng. Part D J. Automob. Eng.*, **233(5)**, pp. 1232–1244, 2019. https://doi.org/10.1177/0954407018766128

[17] Peng, Q., Gui, L. & Fan, Z., Numerical and experimental investigation of splashing oil flow in a hypoid gearbox. *Eng. Appl. Comput. Fluid Mech.*, **12(1)**, pp. 324–333, 2018. https://doi.org/10.1080/19942060.2018.1432506

[18] Dai, Y., Jia, J., Ouyang, B. & Bian, J., Determination of an optimal oil jet nozzle layout for helical gear lubrication: Mathematical modeling, numerical simulation, and experimental validation. *Complexity*, **2020**, 2020. https://doi.org/10.1155/2020/2187027

[19] Santra, T.S., Raju, K., Deshmukh, R., Gopinathan, N., Paradarami, U. & Agrawal, A., Prediction of oil flow inside tractor transmission for splash type lubrication. *SAE Tech. Pap.*, 2019. https://doi.org/10.4271/2019-26-0082

[20] Lu, F., Wang, M., Bao, H., Huang, W. & Zhu, R., Churning power loss of the intermediate gearbox in a helicopter under splash lubrication. *Proc. Inst. Mech. Eng. Part J J. Eng. Tribol.*, 2021. https://doi.org/10.1177/13506501211010030

[21] Deng, X., *et al.*, Lubrication mechanism in gearbox of high-speed railway trains. *J. Adv. Mech. Des. Syst. Manuf.*, **14(4)**, 2020. https://doi.org/10.1299/jamdsm.2020jamdsm0054

[22] Deng, X., Wang, S., Hammi, Y., Qian, L. & Liu, Y., A combined experimental and computational study of lubrication mechanism of high precision reducer adopting a worm gear drive with complicated space surface contact. *Tribol. Int.*, **146**, 2020. https://doi.org/10.1016/j.triboint.2020.106261

[23] Morhard, B., Schweigert, D., Mileti, M., Sedlmair, M., Lohner, T. & Stahl, K., Efficient lubrication of a high-speed electromechanical powertrain with holistic thermal management. *Eng. Res.*, 2020. https://doi.org/10.1007/s10010-020-00423-0

[24] Ji, Z., Stanic, M., Hartono, E.A. & Chernoray, V., Numerical simulations of oil flow inside a gearbox by Smoothed Particle Hydrodynamics (SPH) method. *Tribol. Int.*, **127**, pp. 47–58, 2018. https://doi.org/10.1016/j.triboint.2018.05.034

[25] Liu, H., *et al.*, Numerical modelling of oil distribution and churning gear power losses of gearboxes by smoothed particle hydrodynamics. *Proc. Inst. Mech. Eng. Part J J. Eng. Tribol.*, **233(1)**, pp. 74–86, 2019. https://doi.org/10.1177/1350650118760626

[26] Legrady, B., Taesch, M., Tschirschnitz, G. & Mieth, C.F., Prediction of churning losses in an industrial gear box with spiral bevel gears using the smoothed particle hydrodynamic method. *Eng. Res.*, 2021. https://doi.org/10.1007/s10010-021-00514-6

[27] Mastrone, M.N. & Concli, F., Development of a mesh clustering algorithm aimed at reducing the computational effort of gearboxes' CFD simulations. *Boundary Elements and other Mesh Reduction Methods XLIV*, **131**, pp. 59–69, 2021. https://doi.org/10.2495/be440051

[28] Mastrone, M.N. & Concli, F., CFD simulations of gearboxes: implementation of a mesh clustering algorithm for efficient simulations of complex system's architectures. *Int. J. Mech. Mater. Eng.*, **16(12)**, 2021. https://doi.org/10.1186/s40712-021-00134-6

[29] Mastrone, M. N. & Concli, F., A multi domain modeling approach for the CFD simulation of multi-stage gearboxes. *Energies*, **15(3)**, p. 837, 2022. https://doi.org/10.3390/en15030837

[30] "OpenFOAM." http://www.openfoam.com.

[31] "SALOME." http://www.salome-platform.org.

[32] "Bash." www.gnu.org/software/bash.

[33] Hirt, C. W. & Nichols, B.D., Volume of fluid (VOF) method for the dynamics of free boundaries. *J Comput Phys*, **39(1)**, pp. 201–225, 1981.

[34] Rusche, H., *Computational Fluid Dynamics of Dispersed Two-Phase Flows at High Phase Fractions*. Imperial College of Science, Technology and Medicine, London, 2002.

[35] Kunz, R.F., *et al.*, Preconditioned Navier-Stokes method for two-phase flows with application to cavitation prediction. *Comput. Fluids*, **29(8)**, pp. 849–875.

[36] Höhn, B.R., Michaelis, K. & Otto, H.P., Influences on no-load gear losses. *3rd European Conference on Tribology*, pp. 639–644, 2011.